JOURNAL OF SOLID SATE CHEMISTRY 36, 365–370 (1981)

Electrochemistry of Na_2SO_4 (I) Solid Solutions with Aliovalent Cation Substitution*

H. H. HÖFER AND W. EYSEL†

Institut für Kristallographie, Technische Hochscule, D-5100 Aachen, Germany

AND U. VON ALPEN

Max-Planck-Institut für Festkörperforschung, D-7000 Stuttgart, Germany

Received January 30, 1980; in revised form April 9, 1980

Conductivity data of several Na_2SO_4(I) solid solutions with cation substitutions are presented. The substitution of sodium by bi- and trivalent atoms generates cation vacancy concentrations up to 30% in the structure of Na_2SO_4(I) thus creating high mobility of Na^+. Electrochemical measurements showed that Na^+ ion conductivity prevails and that the electronic partial conductivity is negligible. Complex impedance diagrams were used to determine the influence of the vacancy concentration on the ionic conductivity of Na_2SO_4(I) solid solutions. It was found that the conductivity is strongly correlated to the vacancy concentrations, whereas the size and the charge of the substituting ions show no effect within the accuracy of the measurements. The activation energy as function of the vacancy concentration exhibits a minimum of 0.7 eV at a vacancy concentration of 1%. The maximum of conductivity was found to be $1.5 \times 10^{-2}\ \Omega^{-1}\ cm^{-1}$ at 500°C with 7% vacancies.

Introduction

Sodium sulfate exhibits a complicated polymorphism (*4*). In the high-temperature modification, Na_2SO_4(I), the Na^+ ions can be replaced to a large extent by K^+, Ag^+, Ni^{2+}, Zn^{2+}, Ca^{2+}, Pb^{2+}, Sr^{2+}, Y^{3+}, La^{3+}, Fe^{3+}, etc. (*5*). Of particular crystal chemical and electrochemical interest is the replacement of Na by the aliovalent ions M^{2+} and M^{3+}, which causes up to 30% vacancies ($\square$) in the cation sublattice, described by

$$Na_{2-2x}M_x^{2+}\square_xSO_4$$

and

$$Na_{2-3x}M_x^{3+}\square_{2x}SO_4.$$

In these solid solutions the modification of Na_2SO_4(I) can be stabilized and investigated at room temperature. The crystal structure of these Na_2SO_4(I) solid solutions fulfills one basic condition for the appear-

* This paper forms part of H. H. Höfer's Ph.D. thesis (*1*). A short publication appeared in 1978 (*2*), and a paper was presented at the IUCR meeting in Warsaw 1978 (*3*).

† Present address: Mineralogisch-Petrographisches Institut der Universität, D-6900 Heidelberg, Germany.

0022-4596/81/030365-06$02.00/0

ance of ionic conductivity: the existence of empty sites in at least one sublattice.

In this paper the dependence of the ionic conductivity on vacancy concentration and temperature is reported. Solid solutions in which Na^+ is replaced by Ni^{2+}, Sr^{2+}, Zn^{2+}, and Y^{3+} are studied.

An X-ray structure determination at room temperature based on a model-invariant Fourier synthesis of a Na_2SO_4(I) single crystal (space group $P6_3/mmc$) with composition $(Na_{0.94}Y_{0.02}\square_{0.04})_2SO_4$ leads to ambiguous results (*3*). The tetrahedral structure shows a strong orientational disorder. A more detailed paper on the crystal chemistry and structure of Na_2SO_4(I) is in preparation (Eysel, Höfer, Keester, and Hahn).

Experimental

The starting materials, Na_2SO_4, $ZnSO_4$, $NiSO_4$, $SrSO_4$ from Merck and $Y_2(SO)_4)_3 \cdot 8H_2O$ from Koch–Light, were mixed and heated to the melting point in Pt crucibles. The samples crystallized during quenching in air. The samples' 2ϑ values were checked by X-ray powder diffraction (Norelco diffractometer). The conductivity measurements were carried out using powder pellets pressed with about 8 kbar (6 mm in diameter, 2.5 mm thick, estimated space filling 90–95%) in argon atmosphere.

The partial ionic conductivity was determined by transference experiments and the partial electronic conductivity by polarization measurements. The total conductivity was found via the analysis of complex impedance diagrams.

The cell arrangement for the transference experiment is shown in Fig. 1. Since molten sodium is not in equilibrium with Na_2SO_4 at the experimental temperatures, it was necessary to modify the usual cell arrangement. Between the liquid sodium cathode and the sample a perfectly electronically blocking pellet of β''-Al_2O_3 was placed to prevent the decomposition of Na_2SO_4 into molten Na.

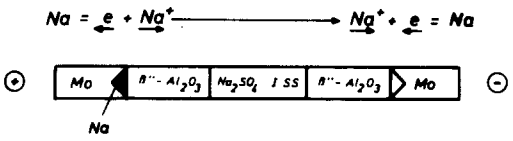

FIG. 1. Electrochemical cell arrangement for the transference experiment of Na_2SO_4(I) solid solutions (ss) with the corresponding electrode reactions.

Moreover, as this material is unstable in contact with sodium, the original Hebb–Wagner polarization experiment with an inert and a reversible electrode could not be carried out. Therefore inert electrodes were used for a polarization experiment to determine the partial electronic conductivity. A cell with the arrangement

$$Au/Na_2SO_4(I)ss/Au$$

based on the perfectly ion blocking effect on gold-sputtered electrodes was used. An identical cell was used for the determination of the total conductivity by the impedance method (*6*).[1] The real and imaginary parts of the impedance were measured in the frequency range 1 Hz to 10 kHz. These measurements were performed using a very low amplitude (3-mV rms).

The impedance data obtained by the frequency response analyzer were processed by an electrochemical data aquisition system (*8*). The calculated impedance data were printed out and the impedance spectrum was plotted on an XY recorder. Data collection, data transfer, analysis, and graphical representation were carried out automatically. The electrolyte resistance was obtained by extrapolating the complex impedance data to the real axis at high frequencies.

[1] The application of powder pellets for impedance measurements is discussed by Armstrong *et al.* (*7*).

Results

Transference experiments at 350°C showed that the transport number for sodium was 1. The experiment was carried out twice. The amount of transported Na was determined by weighing the anode and cathode material and was compared to the transferred charge, resulting in

Transferred charge	7.2	As,	
Transferred amount of Na	1.67	mg,	
Calculated amount of Na	1.77	mg;	(1)
Transferred charge	97.9	As,	
Transferred amount of Na	23.0	mg,	
Calculated amount of Na	23.3	mg.	(2)

At the temperature of operation, the resistance of the β''-alumina pellets is negligible and it was found that the resistance of the cell was comparable to the resistance of the Na_2SO_4 pellet measured using the ac impedance technique between ionically blocking electrodes. This suggests that the Na^+ is the only charge carrier in the Na_2SO_4(I) solid solutions.

X-Ray analysis of the samples before and after the experiments showed that no decomposition of the material had occurred. Polarization between the two inert electrodes of the samples showed that the electronic component was less than 0.1% of the total conductivity in the temperature range 300 to 500°C.

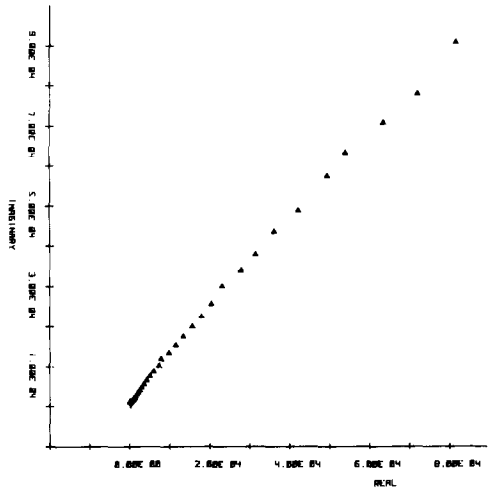

FIG. 2. Impedance diagram of $(Na_{0.84}Y_{0.05}\square_{0.11})_2SO_4$ at 499°C. REAL $= |Z'| \cos \Phi(\Omega)$, IMAGINARY $= -|Z''| \sin \Phi(\Omega)$. Frequency range: 1 Hz–10 kHz.

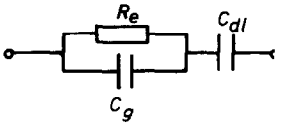

FIG. 3. Equivalent electrical circuit for the solid solutions. R_e = resistance of the electrolyte, C_{dl} = double-layer capacitance, C_g = geometrical capacitance.

A typical impedance of Na_2SO_4(I) doped with 6 mole% $Y_2(SO_4)_3$, i.e., 11% extrinsic cation vacancies, is shown in Fig. 2. A steep increase of the imaginary part of the impedance with decreasing frequency is observed. The maximum available frequency (10 kHz), however, is too low to show the influence of the capacitance parallel to the electrolyte resistance (see the equivalent electrical circuit in Fig. 3). This applies to all measurements included in this paper and is in agreement with computer simulations of the frequency-dependent electrochemical impedance. For these simulations geometrical capacitances of about 10 pF were calculated from known dielectric constants of related compounds such as K_2SO_4, Na_2CO_3, and $CuSO_4$ (9).

From the impedance data linear Arrhenius plots of σT versus $1/T$ (Figs. 4a and b) were obtained for $Na_{2-3x}Y_x^{3+}\square_{2x}SO_4$ solid solutions with varying defect concentrations in the range 0 tp 24% □. It can be seen from Figs. 4a and b that both the conductivity and the activation energy vary with the defect concentration. Similar results were obtained for solid solutions $Na_{2-2x}M_x^{2+}\square_xSO_4$ with M^{2+} = Ni, Zn, and Sr (Table I). The Ni series is shown in Fig. 5.

It can be concluded that, within experi-

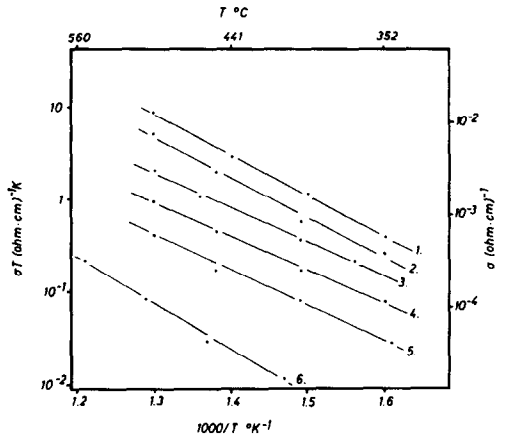

FIG. 4a. Arrhenius plot of $(Na_{2-3x}Y_x\square_{2x})SO_4$. (1) x = 0.019, (2) x = 0.0095, (3) x = 0.0075, (4) x = 0.0050, (5) x = 0.0010, (6) x = 0.0.

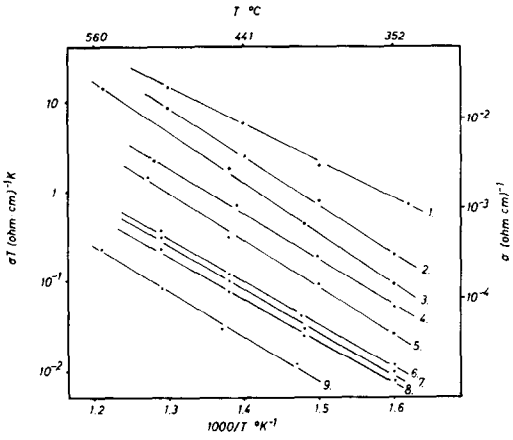

FIG. 4b. Arrhenius plot of $(Na_{2-3x}Y_x\square_{2x})SO_4$. (1) x = 0.037, (2) x = 0.055, (3) x = 0.070, (4) x = 0.084, (5) x = 0.095, (6) x = 0.110, (7) x = 0.115, (8) x = 0.120, (9) x = 0.0.

TABLE I

ELECTROCHEMICAL DATA OF Na_2SO_4(I) SOLID SOLUTIONS

Material	U (eV)	Conductivity (Ω^{-1} cm^{-1}) At 625 K	At 800 K
$Na_{2-3x}M_x\square_{2x}SO_4$			
(1) x = 0.037	0.9	1.4×10^{-3}	2.9×10^{-2}
(2) x = 0.070	1.2	1.4×10^{-4}	1.2×10^{-2}
(3) x = 0.0110	1.0	1.9×10^{-5}	7.4×10^{-4}
(4) x = 0.0	1.0	4.0×10^{-6}	1.8×10^{-4}
$Na_{2-3x}Y_x\square_{2x}SO_4$			
x = 0.001	0.7	5.0×10^{-5}	7.4×10^{-4}
x = 0.005	0.7	1.3×10^{-4}	1.8×10^{-3}
x = 0.009	0.9	4.8×10^{-4}	9.5×10^{-3}
x = 0.055	1.1	3.8×10^{-4}	1.8×10^{-2}
x = 0.120	0.9	1.3×10^{-5}	4.7×10^{-4}
$Na_{2-2x}Sr_x\square_xSO_4$			
x = 0.075	0.9	1.3×10^{-3}	3.7×10^{-2}
x = 0.020	0.8	4.7×10^{-4}	1.1×20^{-2}
x = 0.003	0.7	1.4×10^{-4}	2.3×10^{-3}
$Na_{2-2x}Ni_x\square_xSO_4$			
x = 0.060	0.9	1.2×10^{-3}	3.3×10^{-2}
x = 0.003	0.8	6.4×10^{-5}	1.3×10^{-3}
x = 0.001	1.0	1.7×10^{-5}	7.6×10^{-4}
$Na_{2-2x}Zn_x\square_xSO_4$			
x = 0.100	0.8	4.8×10^{-4}	9.5×10^{-3}
x = 0.060	0.9	3.9×10^{-4}	1.1×10^{-2}
x = 0.020	0.8	2.5×10^{-4}	6.0×10^{-3}

mental error, the conductivity depends only on the number of vacancies and not on the size or valency of the substituting ion. Therefore the conductivity versus the inverse temperature of the various solid-solution series can be represented in the same diagram by using the vacancy concentration as a parameter. Another representation of the results is shown in Fig. 6, with a three-dimensional view shown in Fig. 7.

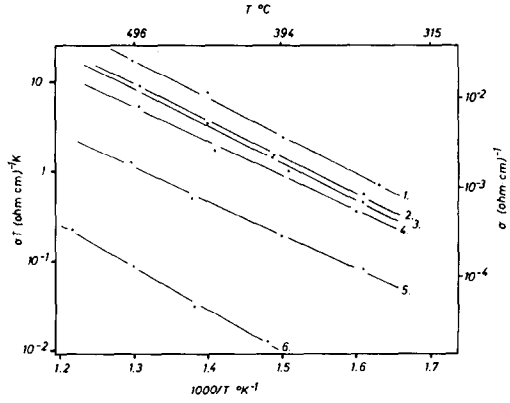

FIG. 5. Arrhenius plot of $(Na_{2-2x}Ni_x\square_x)SO_4$. (1) x = 0.060, (2) x = 0.040, (3) x = 0.005, (4) x = 0.0025, (5) x = 0.005, (6) x = 0.0.

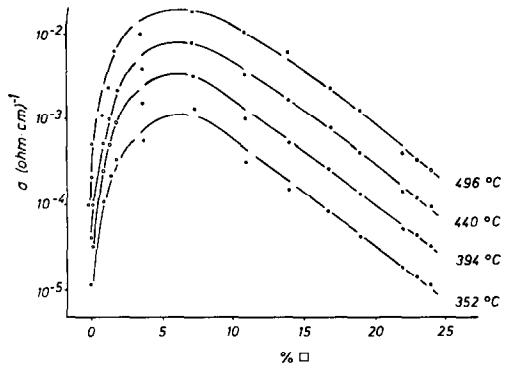

FIG. 6. Isotherms of Na_2SO_4(I)ss conductivity as a function of the vacancy concentration (□).

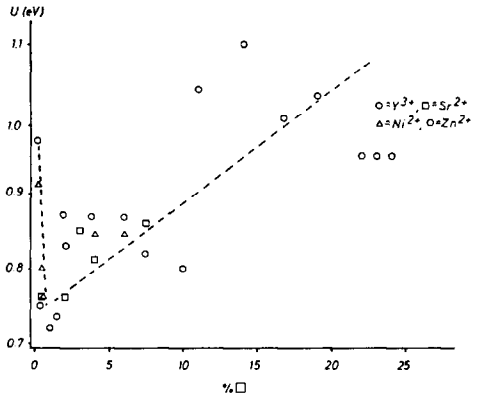

FIG. 8. Activation energy of Na_2SO_4(I)ss versus the vacancy concentration.

The conductivity maximum is independent of temperature and appears at about 7% □. At this maximum the conductivity is 100 times larger than that of pure Na_2SO_4(I). For constant defect concentration the ionic conductivity increases with temperature by two decades between 250 and 500°C. Characteristic values observed are $\sigma = 1.8 \times 10^{-6}\ \Omega^{-1}\ cm^{-1}$ (0% □ at 280°C) and $\sigma = 1.5 \times 10^{-2}\ \Omega^{-1}\ cm^{-1}$ (7.4% □ at 500°C). Thus the range from very low to high ionic conductivity is covered in these solid solutions. (Table I).

Although there is a large spread in the values of the activation energy for sodium ion motion, the results clearly demonstrate a strong decrease at low vacancy concentrations and a subsequent increase (Fig. 8). This implies that the conductivity will be given by an equation of the form

$$\sigma(c) = K \cdot c \cdot \exp\,(U\,(c)/kT),$$

where $U\,(c)$ represents the concentration-dependent activation energy and K is a constant. By inserting the measured values of the activation energy into this equation, it is possible to generate the general form of the conductivity versus concentration curves shown in Fig. 6.

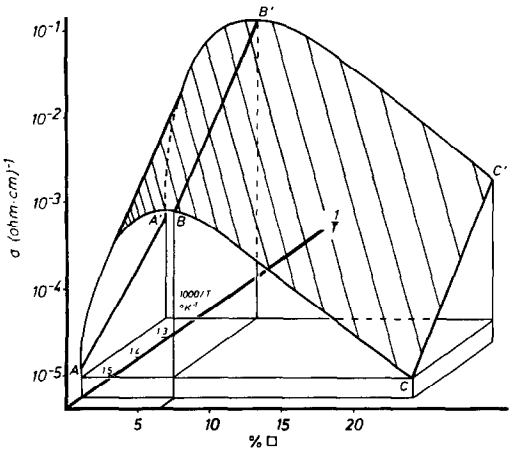

FIG. 7. Conductivity maximum of Na_2SO_4(I)ss.

Discussion

A model based on the mobility of the ions as a function of the defect concentration leads to several structural interpretations. In the simplest case there are no interactions between the mobile Na^+ and the defects (i.e., Y^{3+} and □), in which case a linear relationship exists between the conductivity and the vacancy concentration. This can only be expected at low vacancy concentrations. At high concentrations, when interactions between the defects and Na^+ occur, the situation is more complicated. Now the mobility decreases with increasing interaction.

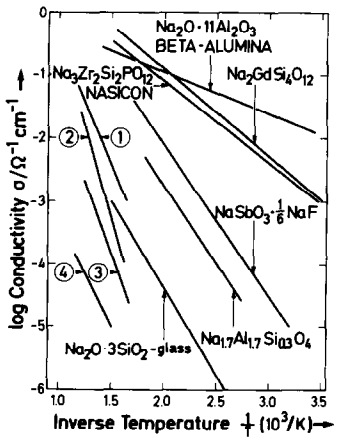

FIG. 9. Na_2SO_4(I)ss with composition $(Na_{2-3x}Y_x\square_{2x})SO_4$ relating to other sodium conductors. (1) $x = 0.037$, (2) $x = 0.070$, (3) $x = 0.110$, (4) $x = 0.0$.

Schmalzried (*10*) has interpreted the conductivity of anion conductors of the ZrO_2ss type. A similar interpretation may be used to explain the present observations on Na_2SO_4(I)ss. With increasing vacancy concentration more migration paths for the sodium ions are created. On the other hand the mobility of the ions is reduced by interactions such as cluster formation (Y^3 □ or □ Y^3 □) and ordering in the cation sublattice. These opposite effects cancel each other at the conductivity maximum at about 7% □. Similar considerations apply for solid solutions with bivalent substituents such as Ni, Zn, and Sr.

A conductivity maximum as described here for Na^+ conduction was described recently for anion conductors with CaF_2 structure by Schmalzried (*10*) and by Reau *et al.* (*11*). In general the activation energy curves are also comparable. The conductivity mechanisms may be similar in these solid solutions with extended and variable vacancy concentrations.

In Fig. 9 we compare the conductivity data of Na_2SO_4(I) solid solutions (Table I) with those of beta-alumina (*12*), $Na_2GdSi_4O_{12}$ (*13*), nasicon (*14*), $NaSbO_3 \cdot \frac{1}{6}NaF$ (*15*), $Na_{1.7}AZ_{1.7}Si_{0.3}O_4$ (*16*) and $Na_2O \cdot 3SiO_2$–glass (*17*). The solid solutions of Na_2SO_4(I) show a rather good Na^+ conductivity, even though not comparable to the very fast conductors BETA ALUMINA (layer structure) or NASICON (channel structure).

Acknowledgments

Helpful discussions with Dr. M. F. Bell, Max-Planck-Institut für Festkörperforschung, Stuttgart, are gratefully acknowledged. We are indebted to the Deutsche Forschungsgemeinschaft and the Max-Planck-Gesellschaft for support.

References

1. H. H. HÖFER, Ph.D. thesis, RWTH Aachen (1979).
2. H. H. HÖFER, W. EYSEL, AND U. VON ALPEN, *Mater. Res. Bull.* **13**, 265 (1978).
3. H. H. HÖFER, U. VON ALPEN, AND W. EYSEL, Eleventh International Congress on Crystallography, Warsaw, August 1978; *Acta Crystallogr. Sect. A* **34**, S358 (1978).
4. B. N. MEHROTRA, H. ARNOLD, TH. HAHN, AND W. EYSEL, *Acta Crystallogr. Sect. A* **31**, S79 (1975).
5. K. L. KEESTER, W. EYSEL, AND TH. HAHN, *Acta Crystallogr. Sect. A* **31**, S79 (1975).
6. R. D. ARMSTRONG, M. F. BELL, AND A. A. METCALFE, *J. Electroanal. Chem.* **77**, 287 (1977).
7. R. D. ARMSTRONG, T. DICKINSON, AND P. W. WILLIS, *Electroanal. Chem. Interf. Electrochem.* **53**, 389 (1974).
8. U. VON ALPEN, K. GRAF, AND M. HAFFENDÖRFER, *J. Appl. Electrochem.* **8**, 557 (1978).
9. "Handbook of Chemistry and Physics," 56th Ed., p. E58, Chem. Rubber Co., Cleveland (1975–1976).
10. H. SCHMALZRIED, *Z. Phys. Chem.* **105**, 47 (1977).
11. J. M. REAU, C. LUCAT, G. CAMPET, J. CLAVERIE, AND J. PORTIER, *Electrochim. Acta* **22**, 761 (1977).
12. M. S. WHITTINGSHAM AND R. A. HUGGINS, *J. Chem. Phys.* **54**, No. 1, 414 (1971).
13. R. D. SHANNON, H.-Y. CHEN, AND T. BERZINS, *Mater. Res. Bull.* **12**, 969 (1977).
14. J. B. GOODENOUGH, H. Y.-P. HONG, AND J. A. KAFALAS, *Mater. Res. Bull.* **11**, 203 (1976).
15. J. SINGER, W. L. FIELDER, H. E. KAUTZ, AND J. S. FORDYCE, *J. Electrochem. Soc.* **123**, 614 (1976).
16. R. D. SHANNON AND T. BERZINS, *Mater. Res. Bull.* **14**, 361 (1979).
17. R. M. KLEIN AND D. A. PLOOF, *Ceram. Bull.* **57**, No. 6, 582 (1978).